N69-20849
NASA CR-100419

U. of Iowa 69-8

Local Time Asymmetries in the Increase of Electron Fluxes in the Outer Van Allen Zone during Substorms*

by

C. S. R. Rao

Department of Physics and Astronomy
THE UNIVERSITY OF IOWA
Iowa City, Iowa

U. of Iowa 69-8

Local Time Asymmetries in the Increase of Electron Fluxes in the Outer Van Allen Zone during Substorms*

by

C. S. R. Rao

Department of Physics and Astronomy
The University of Iowa
Iowa City, Iowa 52240

February 1969

NGL-16-001-002

*This work was supported in part by the National Aeronautics and Space Administration under grant NsG 233-62 and Goddard Space Flight Center under contract NAS5-3097

ABSTRACT

In this paper we study the increase in the fluxes of electrons $E_e \geqslant 40$ keV and $E_e \geqslant 120$ keV in the outer Van Allen zone at different local times during night-time magnetic bay activity. Electrons $E_e \geqslant 40$ keV show increases in the midnight to afternoon sectors but not in the evening sector during bay activity. Electrons $E_e \geqslant 120$ keV do not, however, show significant increases at these times. Also, whereas the increase in the midnight sector occurs immediately after the onset of a bay, a significant increase in the morning sector occurs only later, i.e., during peak or recovery phase of the bay. This time delay is attributed to the time taken by the electrons that are freshly energized in the midnight sector to drift in longitude so as to appear in the morning sector. The absence of increase in the evening sector is believed due to the fact that the freshly energized electrons disappear by the time they drift to that sector.

INTRODUCTION

The morphology of precipitation of energetic electrons in the auroral latitudes has been studied extensively [O'Brien, 1962; O'Brien, 1964; Frank et al., 1964; McDiarmid and Burrows, 1964; Armstrong, 1965]. Based on these and other auroral observations, Hartz and Brice [1967] have shown that there are two distinct zones of precipitation--an intense and discrete precipitation which has a maximum at night and is due to soft electrons (energies of a few keV) and a steady and diffuse precipitation which has a maximum in the morning and is due to harder electrons (energies of a few tens of keV). This division of zones is essentially the same as the one suggested by Piddington [1965]. Recently Jelly and Brice [1967] have observed that the maximum flux of semitrapped and precipitated electrons (as indicated by cosmic noise absorption) in the morning hours in the outer radiation zone is associated with night-time auroral substorms. Hones et al. [1968] have confirmed these observations by using Injun 4 measurements and, in addition, shown that the early evening sector of the outer zone does not respond promptly in this way to a bay. They interpret these results to support the view that electrons which enhance the morning sector of the outer zone are injected by some process acting in the midnight sector of the magnetosphere. Rao [1969a] has analyzed the high latitude flux and cutoff boundary data of energetic electrons in the midnight sector of the outer zone during magnetic bays and has observed that the flux increases without any change in the boundary latitude during the expansive phase of a bay and that, in addition, the boundary extends to higher latitudes during the recovery phase of a bay. Rao [1969b] has also used these data in conjunction with the latitudinal variation of bay activity and concluded that the auroral substorm activity has its onset on closed magnetic field lines in the midnight sector of the magnetosphere. All these observations indicate that auroral events are not isolated phenomena but are part of large scale processes, both spatial and temporal, that take place in the magnetosphere during periods of magnetospheric activity. In this paper we study in detail the local time asymmetries in the increase of electron fluxes in the outer zone during periods of substorm activity for two electron energies and for different altitudes and B values and also discuss the possible reasons for the asymmetry.

INSTRUMENTATION AND DATA

The NASA satellite OGO-C (also known as the first POGO and OGO-II) was launched from the Western Test Range on 14 October 1965 into an orbit of 87° inclination, initial apogee 1514 km, initial perigee 420 km, and a period 104 minutes. The satellite was intended to be fully attitude stabilized with the +Z axis of the spacecraft pointing towards the center of the earth and the X-Y plane parallel to the (horizontal) plane tangent to the earth at the sub-satellite point. However, due to an early failure of the aspect control system such an ideal aspect control could not be achieved and this resulted in a somewhat complex angular motion of the spacecraft. The University of Iowa experiment on this spacecraft comprised four EON type 6213 collimated, directional mica window GM detectors which were designated A1, B1, A2, and B2. The directional geometric factor of each detector was 2.5×10^{-2} cm^2-ster. The energy thresholds were $\sim$ 120 keV for detectors A1 and A2 and $\sim$ 40 keV for the detectors B1 and B2. The collimator axes of A1 and B1 were in the +X direction and those of A2 and B2 in the -Z direction. With these orientations A1 and B1 detectors could be expected to measure mainly the trapped electron fluxes and A2 and B2 detectors to measure precipitating electron fluxes in the auroral latitudes. Due to the angular motion of the satellite data from A1 and B1 detectors showed a number of maxima and minima in the passage of the spacecraft through the inner and outer radiation zones. One could, however, get the smoothed profiles for the two zones by taking the envelope of the maxima. Such fluctuations were generally absent in the data from A2 and B2 detectors. The smoothed profiles obtained from A1 and B1 detectors showed variations similar to the profiles of observed data from A2 and B2 detectors at both quiet and disturbed periods. In the present analysis we have utilized the data from A2 and B2 detectors for the period January-February 1966.

ANALYSIS AND RESULTS

Since we are mainly interested in comparing the flux and the boundary latitude data for the quiet and active periods at different magnetic local times, we have adopted the same method of analysis as the one used by Hones et al. [1968] and represent the data in the form of a series of tables showing the outer zone fluxes and boundary latitudes and a series of figures showing the outer zone electron profiles at different local time periods. The different magnetic local time periods considered are:

(i)	Midnight	(~ 22-23 hrs)
(ii)	Dawn-early morning	(~ 04-07 hrs)
(iii)	Morning-noon	(~ 08-12 hrs)
(iv)	Afternoon	(~ 15-17 hrs)
(v)	Evening	(~ 18-21 hrs)

In each table we list a number of pairs of passes that were either consecutive or separated by only one pass in between. Also, wherever data are available each table is divided into three portions according to whether the pairs of passes occur at a magnetically quiet period or whether the first pass occurs at a quiet time and the second one occurs during the expansive phase or during the recovery phase of a negative bay. In each table we list the day of the year, the UT, the peak fluxes, the boundary latitudes, the altitude and the B value in the outer zone for the two passes and for both the electron energies. We may, however, point out that the absolute values of the peak fluxes as shown in the tables are different on different days since we are tabulating them for different altitudes and B values. Also there have been some continued quiet periods which show very low fluxes and some post-storm but magnetically quiet periods which show high fluxes. However, since we are comparing the fluxes during quiet periods and periods of bay activity, this is not of much concern and it only illustrates that the effects we are seeking occur at different altitudes and B values. The values of the boundary latitudes shown in the table correspond to those where the count rates come down to 10 c/s. The possibility that these values may not give a correct idea about the boundary due to angular motion of the satellite has been considered. However, since we have seen that, in a large number of instances (not cited in the paper) such values are very consistent, we believe that they are trustworthy. In each figure we have shown the variation of the apparent count rate with the invariant latitude and the peak flux shown in the tables have been obtained by converting the peak apparent count rate to true count rate by using laboratory calibration curves and then dividing this value by the geometric factor. Also, in each figure Pass 1 shows the quiet time pass and Pass 2 the succeeding pass either at quiet time or during a bay. The stations whose magnetograms are used in this paper are listed in Table I. We analyze below the data for the different time periods.

Midnight Sector Passes: In Table 2 we list data for a number of pairs of passes in this sector. From the data, we observe the following:

(i) For pairs of passes during quiet time there is, in general, no significant difference between either the fluxes or the boundary latitudes for both energy thresholds. Figure 1 shows one pair of such passes on 18 January MLT ~ 23 hours. It would be observed that not only are the fluxes the same but that the whole outer zone profiles are very similar.

(ii) During the expansive phase of a bay, the peak flux of electrons $E_e \geqslant 120$ keV does not show much change but that of electrons $E_e \geqslant 40$ keV shows a large increase above an invariant latitude of $\sim 65°$ and the boundary latitudes are similar to those of quiet time. Figure 2 illustrates one pair of such passes on 4 February for an MLT ~ 22 hours, in which Pass 1 occurs at quiet time and Pass 2 during the expansive phase of a bay at Fort Churchill. An increase of about 2° in the boundary latitude for electrons $E_e \geqslant 120$ keV during the bay is not considered significant since it is within the variations between two consecutive passes during quiet periods.

(iii) During the recovery phase of a bay there is an extension of the boundary for electrons $E_e \geqslant 40$ keV to higher latitudes in addition to the large increase in peak flux; however, for electrons $E_e \geqslant 120$ keV, extension of the boundary is observed but without any appreciable changes in the peak flux. Figure 3 shows a pair of passes on 6 February for an MLT ~ 22 hours in which the extension of the boundary for both electron energy thresholds and the flux increase for electrons $E_e \geqslant 40$ keV above an invariant latitude ~ 65° are clearly seen.

Dawn-Early Morning Passes: Passes between 04-07 MLT are listed in Table III. Unfortunately, no data are available during the expansive phase of bays for the period so we list passes for the quiet periods and for the recovery phase of bays. The observations for this MLT period are as follows:

(i) During quiet time the fluxes remain similar for both passes of the pair and the boundary latitudes are within about 2°-3° for both energy thresholds. Figure 4 illustrates one pair of passes for an MLT ~ 07 hours on 28 January. It would be seen that the outer zone profiles are almost the same for both the passes.

(ii) In Fig. 5 we illustrate a set of passes for an MLT ~ 05 hours in which Pass 1 is a quiet time pass and Pass 2 occurs during the recovery phase of a bay at Fort Churchill on 6 February.

No change in flux is observed for electrons $E_e \geqslant 120$ keV whereas there is an increase for electrons $E_e \geqslant 40$ keV above an invariant latitude $\sim 65°$. Boundary changes are also not significant.

Morning-Noon Passes: Table IV shows pairs of passes between the MLT period 08-12 hours. From this table we observe the following:

(i) During quiet time the peak fluxes of electrons are similar and the variations in boundary latitudes are $\sim 2°$-$3°$ for successive passes for electrons of both energy thresholds. An illustration for an MLT $\sim$ 11 hours on 18 January is given in Fig. 6, in which it would be seen that the profiles are very similar.

(ii) During the expansive phase of a bay the position is similar to that during quiet time. An example of this is shown for an MLT $\sim$ 11 hours in Fig. 7 in which Pass 1 occurs during quiet time and the next Pass 2 during the expansive phase of a bay at Fort Churchill on 20 January.

(iii) During the recovery phase of a bay there is no significant change in either the peak flux or boundary latitude for electrons $E_e \geqslant 210$ keV and while there is a large increase in the peak flux for electrons $E_e \geqslant 40$ keV, the changes in the boundary latitude are not very consistent though there is a tendency for an increase. Figure 8 shows one pair of passes on 4 February in which Pass 2 occurs during the recovery phase of a bay at Great

Whale River and at Fort Churchill. The flux increase for electrons $E_e \geqslant 40$ keV above an invariant latitude $\sim 65°$ is clearly seen.

Afternoon Passes: Pairs of passes during quiet time are listed in Table V. No data are available for passes during bays. The data for quiet time have, however, been listed to show the similarity between the fluxes and the boundary latitudes for electrons of both energy thresholds for two successive passes.

Evening Passes: Passes for the MLT period 18-21 hours are listed in Table VI from which we observe the following:

(i) During quiet time the variations in the peak fluxes and boundary latitudes for both energy thresholds are the same as those for other quiet local time periods, as could be seen in Fig. 9 for a pair of passes at an MLT $\sim$ 19 hours on 24 January.

(ii) During the expansive or the recovery phases of bays, no significant change as compared to quiet time is observed either in fluxes or in boundary latitudes. This is illustrated in Fig. 10 for an MLT $\sim$ 21 hours on 26 January, in which Pass 2 occurs during the recovery of a strong bay at College. In fact, the flux in Pass 2 is less than that during the quiet time for Pass 1.

CONCLUSIONS

In the previous section we have seen that the flux of electrons $E_e \geqslant 40$ keV in the midnight sector of the outer Van Allen belt shows a significant increase without any increase in the boundary latitude during the expansive phase of a bay; and, during the recovery phase of a bay there is, in addition, an extension of the boundary to higher latitudes. The fact that there is no apparent time delay between the beginning of a substorm and the sudden appearance of large fluxes of electrons in the outer zone and that the extension in boundary latitude comes about only at a later stage of the bay confirm the earlier conclusions obtained from Injun 4 [Rao, 1969a] that the mechanism of magnetic field line merging may not play a primary role in the production of energetic auroral particles and that a local acceleration mechanism acting in the midnight sector of the outer zone provides a source for the energetic particles there. Similar conclusions were reached by Hones et al. [1968] who used simultaneous measurements of electrons from the Vela and the Injun 4 satellites.

We have also observed that the flux of electrons $E_e \geqslant 120$ keV in the midnight sector of the outer zone does not show significant increases but that, at times, the boundary does extend to higher latitudes. If, as we have stated above, the increased flux of electrons $E_e \geqslant 40$ keV is due to energization of low energy electrons in the midnight sector, then the fact that the flux of electrons $E_e \geqslant 120$ keV does not increase during the bay indicates that the total energy changes in these processes are comparatively small.

Regarding morning-noon observations, we have noted that a significant increase in the flux of electrons $E_e \geqslant 40$ keV occurs during the recovery phase of a bay but not during the expansive phase. There is thus a time delay between the appearance of increased flux in the midnight sector and in the morning sector. In order to explain this delay, let us consider the time history of a substorm. According to Akasofu [1964] an auroral substorm has a lifetime of 1-3 hours and consists of two phases and it always originates around the midnight meridian. The first or the expansive phase lasts up to ~ 30 minutes and the second or the recovery phase up to ~ 3 hours. Our observations of the substorms considered in this paper indicate that the recovery period starts after ~ 30-45 minutes after the beginning of a substorm. This period is about the time taken by electrons $E_e \geqslant 40$ keV to drift in longitude from the midnight sector to the daytime sector. We, therefore, attribute the delayed appearance of the increased flux in the morning sector to the time taken by the electrons that are freshly energized in the midnight sector during the expansive phase of a substorm to drift in longitude so as to appear in that sector.

Considering the evening sector we believe that the absence of increases in that sector is due to the fact that the freshly energized electrons probably disappear by the time they drift to that sector.

TABLE I

Station	Magnetic Latitude (deg.)	Approx. Magnetic Local Time (MLT) of Station at Zero Hours (U.T.)
Leirvogur, Iceland	70.2	0
Kiruna, Sweden	65.3	3
Barrow, Alaska	68.5	11
College, Alaska	64.6	12
Fort Churchill, Canada	68.7	17
Great Whale River, Canada	66.6	18

TABLE II

Day 1966	1st Pass UT	2nd Pass UT	MLT	1st Flux $\times 10^4$	2nd Flux $\times 10^4$	1st Boundary Inv. Lat.	2nd Boundary Inv. Lat.	1st Flux $\times 10^4$	2nd Flux $\times 10^4$	1st Boundary Inv. Lat.	2nd Boundary Inv. Lat.	Altitude (km)	B (gauss)
				← > 120 keV electrons →				← > 40 keV electrons →					
						MIDNIGHT SECTOR PASSES							
						(a) Quiet Time							
1/17	16.7	20.2	22	3.3	3.2	69.2	69.4	1.4	1.4	71.2	70.4	1350	.31
1/18	17.1	18.8	22	0.3	0.1	65.6	65.2	0.5	0.3	71.7	73.0	1320	.32
1/24	2.6	4.3	22	3.1	2.4	67.9	68.0	11.0	7.8	69.0	69.1	550	.44
1/27	8.8	10.5	22	6.0	9.2	69.0	67.0	3.0	4.6	69.0	69.9	490	.52
1/28	7.4	9.1	22	0.3	0.2	68.9	68.6	0.7	0.6	69.3	68.6	525	.50
1/19	2.5	4.2	22	0.08	0.07	67.0	66.8	1.3	1.3	70.1	69.0	480	.45
1/18	3.9	5.6	23	0.2	0.2	67.8	68.2	0.7	0.5	69.3	68.6	470	.46
1/19	4.2	5.9	23	0.07	0.08	66.8	67.6	1.3	2.1	69.0	69.8	475	.46
						(b) During Expansive Phase of Bays							
2/4	4.8	8.2	22	1.5	2.4	67.3	69.9	5.6	34.0	69.6	70.1	700	.45
1/23	3.9	5.7	23	2.0	1.5	67.9	67.9	6.4	> 10.0	69.6	69.1	530	.45
						(c) During Recovery Phase of Bays							
2/5	3.4	5.2	22-23	0.9	1.0	67.8	72.4	2.8	34.0	70.4	73.1	900	.36
2/6	5.5	7.2	22-23	1.1	0.8	66.2	71.5	4.3	21.0	68.0	73.7	750	.44
1/9	20.8	22.5	23	0.3	0.4	65.0	69.2	1.0	4.6	66.6	75.2	1450	.30
1/19	7.7	11.1	23	0.03	0.03	68.2	67.6	0.6	4.0	71.3	75.7	450	.52
1/24	7.6	9.4	23	1.6	0.6	66.9	69.8	5.8	18.0	68.2	72.6	480	.51

TABLE III

Day 1966	1st Pass UT	2nd Pass UT	MLT	1st Flux x 10^4	2nd Flux x 10^4	1st Boundary Inv. Lat.	2nd Boundary Inv. Lat.	1st Flux x 10^4	2nd Flux x 10^4	1st Boundary Inv. Lat.	2nd Boundary Inv. Lat.	Altitude (km)	B (gauss)
				← > 120 keV electrons →				← > 40 keV electrons →					
DAWN--EARLY MORNING PASSES													
(a) Quiet Time													
2/26	0.8	2.5	03-04	5.1	6.8	70.6	70.2	9.6	12.0	73.6	72.2	1500	.28
1/27	7.2	8.9	04	2.6	2.8	69.0	70.3	6.0	6.8	71.5	72.9	700	.40
2/4	4.9	6.6	04	2.9	3.2	70.1	68.8	11.0	14.0	71.9	71.0	1000	.33
2/28	8.4	10.1	04-05	5.4	5.0	69.7	70.5	9.2	7.7	72.4	73.0	1500	.30
1/25	9.4	11.7	05	2.6	3.1	71.3	72.2	7.6	7.4	76.2	78.1	620	.45
2/26	11.9	13.6	05	2.5	2.3	69.7	70.3	5.3	6.0	77.4	74.6	674	.44
1/27	18.4	20.2	06	4.3	4.1	70.5	70.0	11.0	9.6	73.7	73.0	1380	.32
1/28	17.0	20.5	06	3.8	4.8	73.4	71.8	7.2	8.8	75.9	76.4	1350	.33
1/25	19.4	21.2	06-07	3.8	4.0	71.9	69.5	13.0	11.0	79.2	77.1	1400	.32
2/27	0.1	1.9	06-07	0.6	0.5	69.3	69.5	2.3	2.2	71.2	75.2	560	.45
2/28	17.2	19.0	06-07	2.7	3.0	70.2	70.1	5.8	5.7	73.0	73.0	1530	.33
1/17	18.2	20.0	07	0.4	0.4	71.7	71.3	1.8	2.1	74.4	73.7	1500	.31
1/18	18.6	22.1	07	0.2	0.2	68.8	68.7	3.0	3.2	73.5	75.2	1500	.31
1/25	21.2	22.9	07	4.0	4.2	69.5	70.8	11.0	11.0	77.1	76.5	1380	.33
1/28	0.7	2.4	07	1.6	1.8	70.4	70.5	4.3	4.5	73.4	72.6	940	.38
2/26	12.9	14.6	07	6.0	5.8	72.9	73.7	12.0	12.0	76.5	79.8	1480	.32
(b) During Recovery Phase of Bays													
2/6	5.7	7.3	04	3.7	3.5	68.0	69.6	12.0	28.0	70.9	71.0	1000	.33
2/5	3.6	5.3	04-05	1.5	3.4	68.5	71.0	11.0	52.0	72.5	72.7	1000	.34
1/24	7.6	9.6	05	3.4	3.5	70.1	70.5	6.1	44.0	72.6	75.1	620	.42
1/19	6.1	7.8	05-06	0.05	0.09	67.9	69.1	0.9	4.0	71.6	70.5	575	.40
1/25	6.5	8.2	05-06	2.6	2.2	70.0	71.2	6.7	34.0	70.6	73.2	700	.38
2/6	2.3	3.9	05-06	3.3	4.8	67.9	69.1	12.0	18.0	71.6	71.7	1100	.32
1/19	9.5	11.2	06	0.1	0.2	68.6	70.4	2.8	29.0	72.7	74.5	525	.45
1/20*	9.8	8.1	06	0.1	0.3	68.8	67.6	1.5	20.0	74.4	72.4	550	.42
2/10	20.1	21.8	06	0.6	0.8	68.3	68.0	1.5	12.0	77.4	76.4	1000	.37
2/10-2/11	22.9	2.3	06-07	0.9	1.2	68.0	67.9	2.6	24.0	74.9	70.5	1330	.33

*First pass after the second

TABLE IV

Day 1966	1st Pass UT	2nd Pass UT	MLT	1st Flux x 10^4	2nd Flux x 10^4	1st Boundary Inv. Lat.	2nd Boundary Inv. Lat.	1st Flux x 10^4	2nd Flux x 10^4	1st Boundary Inv. Lat.	2nd Boundary Inv. Lat.	Altitude (km)	B (gauss)
				← > 120 keV electrons →				← > 40 keV electrons →					
MORNING--NOON PASSES													
(a) Quiet Time													
1/22	2.0	3.7	07-08	1.8	1.7	69.7	71.0	7.2	5.6	74.5	73.1	750	.40
2/26	3.3	5.0	08	1.0	1.3	71.5	71.1	3.1	2.6	> 74.3	76.4	580	.43
1/25	0.3	2.0	08-09	3.4	3.5	71.0	69.3	11.0	9.2	79.6	75.4	1375	.33
1/27	13.1	14.9	08-09	4.4	4.2	71.3	70.7	11.0	11.0	73.6	76.1	1450	.32
1/27	14.1	15.9	08-09	2.4	2.2	71.6	71.3	6.0	5.5	74.7	76.3	700	.43
1/25	2.0	3.8	09-10	3.5	3.3	69.3	70.9	9.2	11.0	75.4	75.6	1400	.32
1/26	2.4	4.1	09-10	4.8	4.3	70.5	70.7	9.6	11.0	75.9	76.2	1350	.33
1/18	16.1	17.9	10	0.1	0.1	70.4	69.6	0.5	0.5	75.0	75.1	540	.47
1/24	3.4	5.2	10	4.0	4.7	70.9	70.8	11.0	12.0	74.9	74.0	1400	.32
1/27	9.7	11.4	10-11	4.0	3.7	71.4	71.8	10.0	9.6	76.7	75.8	1400	.31
1/18	4.7	6.4	11	0.4	0.4	70.8	70.4	1.7	1.6	73.2	74.6	1500	.30
1/27	4.5	8.0	11	3.5	3.8	73.4	71.4	12.0	9.2	77.2	76.8	1350	.33
1/28	8.4	10.0	11-12	3.1	3.2	71.0	71.6	6.9	6.8	76.6	76.2	1360	.31
1/18	8.2	9.9	12	0.4	0.4	70.3	71.7	1.3	1.7	73.8	77.0	1500	.30
(b) During Expansive Phase of Bays													
2/19	12.1	13.8	08	0.5	0.5	70.6	72.6	4.2	4.8	74.3	75.5	1350	.32
1/20	3.7	7.2	11	0.2	0.2	68.6	68.5	2.1	2.2	75.2	74.5	1500	.31
1/19	8.5	10.3	12	0.2	0.2	68.7	68.9	2.1	1.3	74.6	74.7	1500	.29
(c) During Recovery Phase of Bays													
1/23	12.7	14.4	07-08	2.1	2.1	72.8	72.0	8.8	16.0	76.0	78.6	600	.45
1/23	13.4	15.2	08-09	4.6	6.0	69.4	72.4	16.0	52.0	72.2	76.8	1500	.31
1/26*	14.5	12.8	08-09	3.2	4.8	72.7	74.5	12.0	52.0	79.5	78.6	1450	.32
1/9	20.5	22.3	08-09	0.3	1.0	68.9	--	4.4	42.0	78.2	76.5	1500	.31
1/20	10.6	14.0	10-11	0.2	3.8	69.3	71.4	3.3	48.0	75.4	74.8	1500	.30
2/5	4.3	6.1	10-11	1.7	3.1	72.4	74.4	18.0	36.0	75.5	76.4	1050	.35
2/4	7.4	9.2	11	1.7	1.9	69.8	72.2	8.8	26.0	75.4	75.2	1200	.33
1/24	8.5	10.3	11	4.9	4.3	71.2	72.8	9.6	25.0	75.7	74.2	1450	.31
1/25	7.3	9.0	11-12	3.0	2.8	71.3	75.1	9.2	24.0	76.1	79.5	1400	.32
1/22	4.4	7.9	12	6.0	4.3	71.3	74.7	16.0	40.0	76.2	77.0	1400	.31
1/20	7.2	8.9	12	0.2	0.3	68.5	72.9	2.2	14.0	74.5	79.0	1500	.30

*First pass after the second

TABLE V

Day 1966	1st Pass UT	2nd Pass UT	MLT	1st Flux $\times 10^4$	2nd Flux $\times 10^4$	1st Boundary Inv. Lat.	2nd Boundary Inv. Lat.	1st Flux $\times 10^4$	2nd Flux $\times 10^4$	1st Boundary Inv. Lat.	2nd Boundary Inv. Lat.	Altitude (km)	B (gauss)
				← > 120 keV electrons →				← > 40 keV electrons →					
				AFTERNOON PASSES--Quiet Time									
2/26	1.7	5.1	15	1.3	1.4	73.4	72.1	6.2	4.0	75.1	76.3	450	4.8
2/26	14.5	18.0	16	4.8	6.6	72.1	70.3	8.4	12.0	77.7	75.1	1350	3.0
2/26	18.0	19.8	16	6.6	6.4	70.3	70.1	11.0	11.0	75.1	72.5	1390	.30
2/27	18.4	20.1	16	5.0	5.1	69.9	70.0	8.4	8.4	74.2	73.6	1420	29
1/28	17.9	21.4	17	1.7	2.4	72.5	70.0	3.1	4.7	75.8	75.5	600	.41
2/19	9.6	11.3	17	1.6	1.6	71.1	70.3	3.0	2.0	74.7	74.2	560	.45
2/21	6.8	8.6	17	1.2	0.8	69.5	69.2	4.9	2.8	73.9	72.9	480	.46
2/21	16.1	17.8	17	3.8	4.3	71.0	71.8	8.4	9.9	74.5	75.1	1050	.29

TABLE VI

Day 1966	1st Pass UT	2nd Pass UT	MLT	1st Flux x 10^4	2nd Flux x 10^4	1st Boundary Inv. Lat.	2nd Boundary Inv. Lat.	1st Flux x 10^4	2nd Flux x 10^4	1st Boundary Inv. Lat.	2nd Boundary Inv. Lat.	Altitude (km)	B (gauss)
				← > 120 keV electrons →				← > 40 keV electrons →					
						EVENING PASSES							
						(a) Quiet Time							
1/24	3.7	5.4	18	3.6	3.1	70.2	69.0	10.0	6.2	73.6	71.2	1100	.37
2/26	12.1	13.8	18	0.5	0.5	69.2	68.8	1.4	2.3	74.0	74.1	450	.46
1/25	9.2	10.9	18-19	4.0	4.4	71.7	70.5	12.0	14.0	73.4	72.6	1200	.35
1/24	21.7	23.4	19	2.2	1.9	68.7	68.4	5.7	5.3	70.6	69.4	560	.42
2/27	14.2	17.6	19	6.2	3.6	69.3	69.4	2.3	1.4	71.5	72.3	440	.44
1/27	14.0	15.7	19-20	3.2	4.4	67.5	68.6	1.2	1.6	69.9	70.5	470	.45
2/19	8.4	10.1	19-20	0.2	0.2	69.9	69.5	2.7	1.8	71.8	71.8	980	.42
1/18	11.8	13.6	20	0.3	0.3	69.9	69.9	1.5	1.3	71.8	70.0	1350	.33
1/19	0.1	1.9	20-21	0.2	0.2	68.4	68.5	3.2	2.6	71.2	71.6	1200	.34
1/27	13.4	16.9	20-21	1.8	1.4	69.9	69.4	5.2	3.5	72.0	70.2	1100	.35
1/27	22.1	23.9	20-21	2.5	2.7	70.7	70.7	5.3	6.6	72.3	72.5	1000	.36
1/28	0.6	2.3	20-21	1.6	1.0	69.9	68.8	3.7	2.5	71.4	71.3	640	.42
1/28	17.2	20.7	21	1.9	2.5	71.7	69.6	4.0	4.2	73.5	72.9	1000	.35
						(b) During Expansive Phase of Bays							
1/22	4.7	6.4	18	4.1	2.5	72.2	73.1	14.0	5.6	74.6	74.1	1200	.35
2/6	2.0	3.7	21	1.6	1.4	66.7	66.3	5.7	4.2	67.7	69.9	800	.38
						(c) During Recovery Phase of Bays							
1/23	5.0	6.7	18	5.0	3.6	70.2	73.4	14.0	11.0	72.3	73.8	1200	.35
1/24	7.1	10.6	18-19	3.8	3.3	70.6	67.6	10.0	11.0	73.1	73.6	1200	.35
2/10	20.9	22.9	18-19	1.0	1.3	67.0	66.4	1.9	2.8	68.6	68.7	950	.34
1/20	4.0	7.4	19	1.4	1.1	67.5	66.2	15.0	6.0	68.3	67.8	1200	.33
1/26	9.6	13.0	19-20	3.5	2.4	69.5	71.0	10.0	5.5	74.0	72.0	1160	.35
1/20	10.9	14.3	20-21	0.1	0.1	66.9	65.1	1.2	1.0	68.1	70.1	1300	.33
1/23	12.0	13.7	20-21	4.4	2.7	68.6	65.3	12.0	5.7	72.3	68.4	1200	.35
1/20	14.3	16.1	21	0.1	0.1	65.1	63.6	0.9	0.8	70.1	71.7	1300	.33

ACKNOWLEDGEMENTS

My grateful thanks are due to Professor J. A. Van Allen who provided me the opportunity to work in this laboratory and took a keen interest in the present work. This research was supported in part by the National Aeronautics and Space Administration under grant NsG 233-62 and Goddard Space Flight Center under contract NAS5-3097.

REFERENCES

Akasofu, S.-I., The development of the auroral substorm, Planetary Space Sci., 12, 273-282, 1964.

Armstrong, T., Morphology of the outer zone electron distribution at low latitudes from January through July and September 1963 from Injun 3, J. Geophys. Res., 70, 2077-2110, 1965.

Frank, L. A., J. A. Van Allen, and J. D. Craven, Large diurnal variations of geomagnetically trapped and of precipitated electrons observed at low latitudes, J. Geophys. Res., 69, 3155-3167, 1964.

Hartz, T. R., and N. M. Brice, The general pattern of auroral particle precipitation, Planetary Space Sci., 15, 301-329, 1967.

Hones, E. W., Jr., S. Singer, and C. S. R. Rao, Simultaneous observations of electrons ($E > 45$ keV) at 2000 kilometers altitude and at 100,000 kilometers in the magnetotail, J. Geophys. Res., 73, 7339-7359, 1968.

Jelly, Doris, and Neil Brice, Changes in Van Allen radiation associated with polar substorms, J. Geophys. Res., 72, 5919-5931, 1967.

McDiarmid, I. B., and J. R. Burrows, Diurnal intensity variations in the outer radiation zone at 1000 km, Can. J. Phys., 42, 1135-1148, 1964.

O'Brien, B. J., Lifetimes of outer-zone electrons and their precipitation into the atmosphere, J. Geophys. Res., 67, 3687-3706, 1962.

O'Brien, B. J., High-latitude geophysical studies with satellite Injun 3. 3. Precipitation of electrons into the atmosphere, J. Geophys. Res., 69, 13-43, 1964.

Piddington, J. H., The morphology of auroral precipitation, Planetary Space Sci., 13, 565-577, 1965.

Rao, C. S. R., Some observations of energetic electrons in the outer radiation zone during magnetic bays, J. Geophys. Res., 74, 794-801, 1969(a).

Rao, C. S. R., Some observations on energetic electrons in the outer Van Allen zone during auroral substorms in relation to open and closed field lines, U. of Iowa Research Report 68-66, 1968 [submitted to J. Geophys. Res. for publication], 1969(b).

FIGURE CAPTIONS

Figure 1. Two consecutive quiet time passes of OGO-C in the midnight sector of the outer Van Allen zone on 18 January.

Figure 2. A pair of passes of OGO-C in the midnight sector of the outer Van Allen zone on 4 February. Pass 1 occurs during quiet time and Pass 2 occurs during the expansive phase of a bay at Fort Churchill.

Figure 3. A pair of passes of OGO-C in the midnight sector of the outer Van Allen zone on 6 February in which Pass 1 occurs at a quiet time and Pass 2 during the recovery phase of a bay at Fort Churchill.

Figure 4. Two successive quiet time passes of OGO-C in the early morning sector of the outer Van Allen zone on 28 January.

Figure 5. Two successive passes of OGO-C in the early morning sector of the outer Van Allen zone on 6 February in which Pass 1 is a quiet time pass and Pass 2 occurs during the recovery phase of a bay at Fort Churchill.

Figure 6. Two consecutive quiet time passes of OGO-C in the late morning sector of the outer zone on 18 January.

Figure 7. A pair of passes of OGO-C in the late morning sector of the outer Van Allen zone on 20 January. Pass 1 occurs

during quiet time and Pass 2 during the expansive phase of a bay at Fort Churchill.

Figure 8. A pair of passes of OGO-C in the late morning sector of the outer Van Allen zone on 4 February in which Pass 1 occurs at quiet time and Pass 2 during the recovery phase of a bay at Great Whale River and Fort Churchill.

Figure 9. A pair of quiet time passes of OGO-C in the evening sector of the outer Van Allen zone on 24 January.

Figure 10. A pair of passes of OGO-C in the evening sector of the outer Van Allen zone on 26 January in which Pass 1 occurs at quiet time and Pass 2 during the recovery phase of a bay at College.

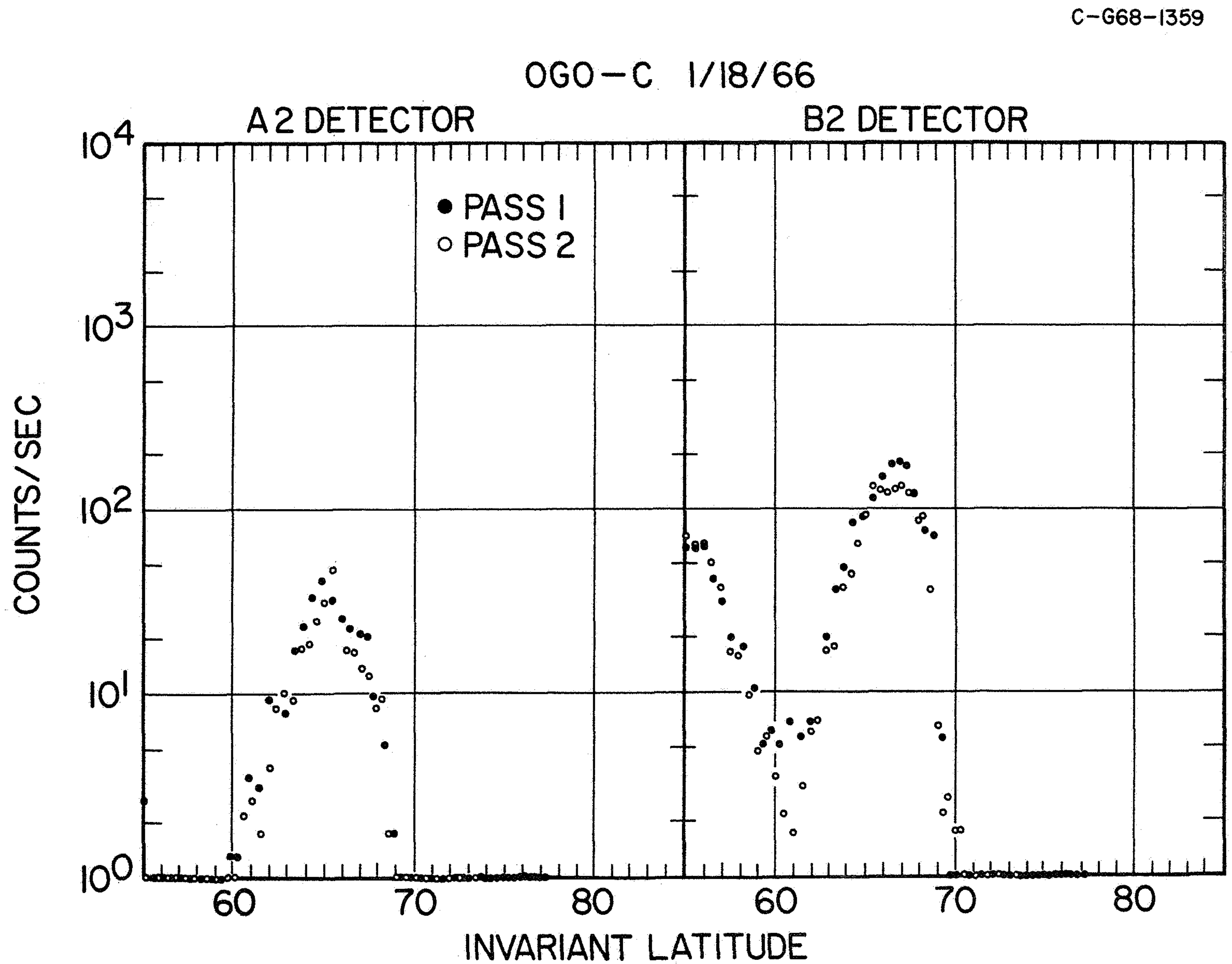
C-G68-1359
OGO—C 1/18/66
A2 DETECTOR
B2 DETECTOR
PASS 1
PASS 2
COUNTS/SEC
10^4
10^3
10^2
10^1
10^0
60
70
80
60
70
80
INVARIANT LATITUDE

Figure 1

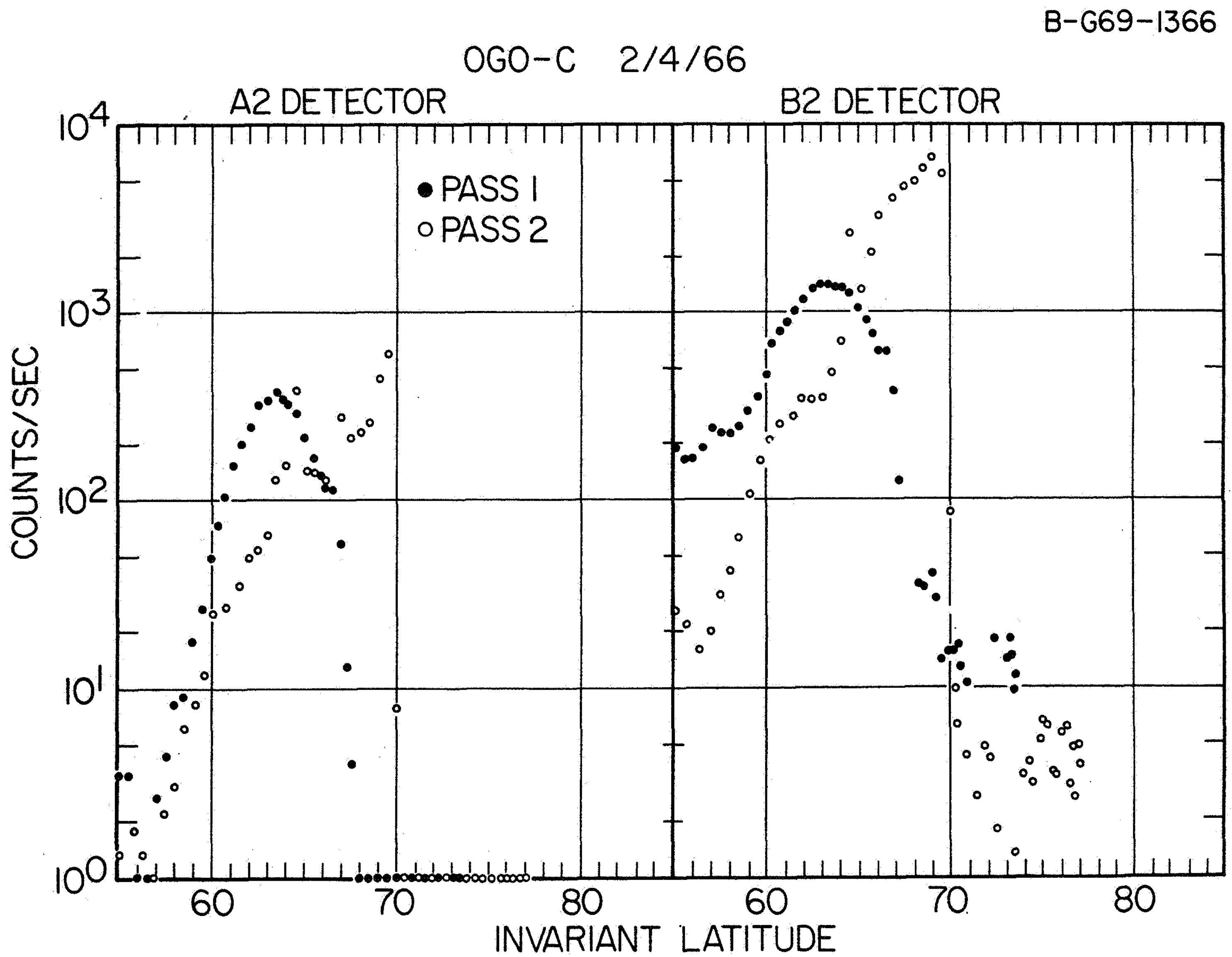
B-G69-1366
OGO-C 2/4/66
A2 DETECTOR
B2 DETECTOR
PASS 1
PASS 2
COUNTS/SEC
10^4
10^3
10^2
10^1
10^0
60
70
80
60
70
80
INVARIANT LATITUDE

Figure 2

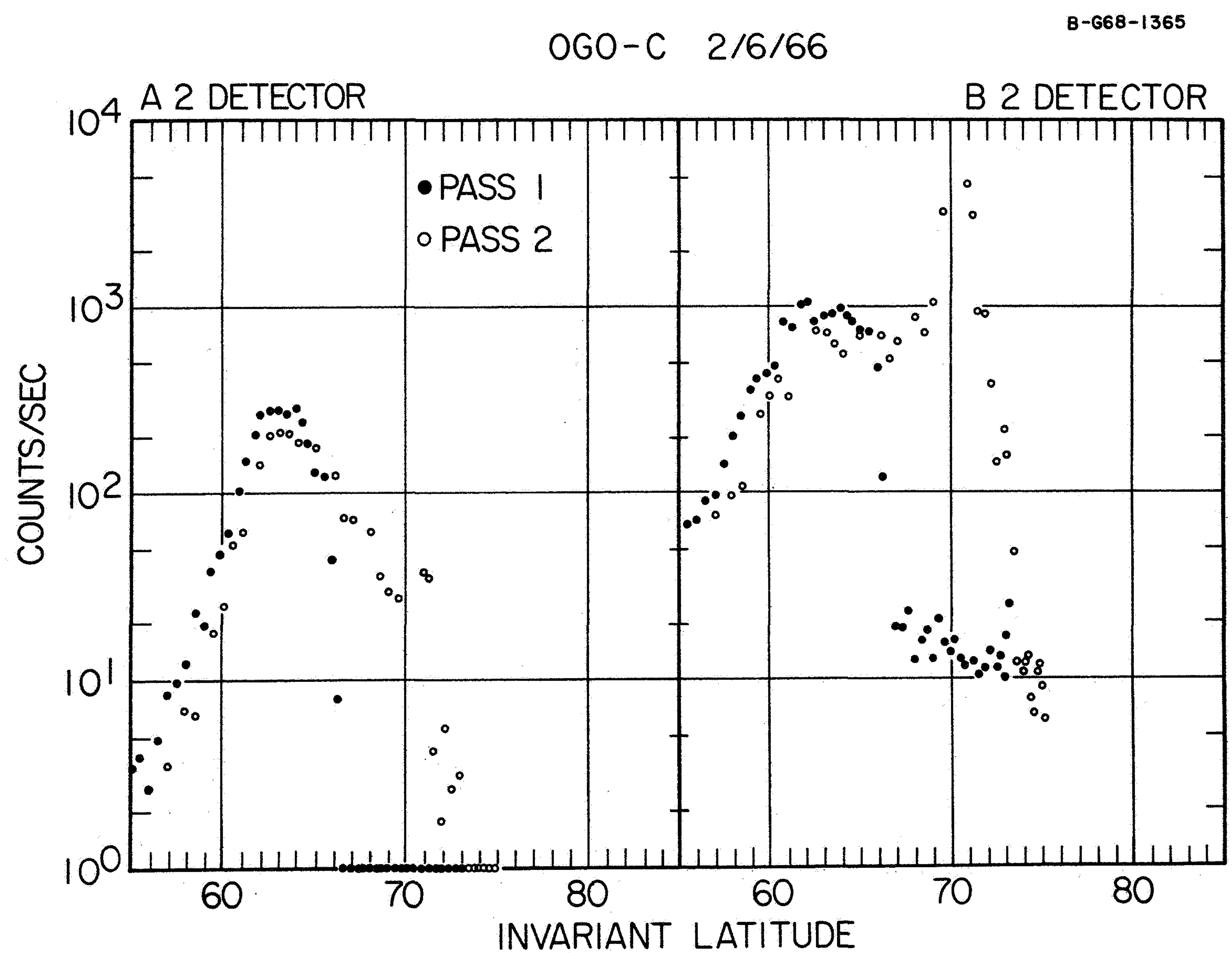
B-G68-1365
OGO-C 2/6/66
A 2 DETECTOR
B 2 DETECTOR
PASS 1
PASS 2
COUNTS/SEC
10^4
10^3
10^2
10^1
10^0
60
70
80
INVARIANT LATITUDE

Figure 3

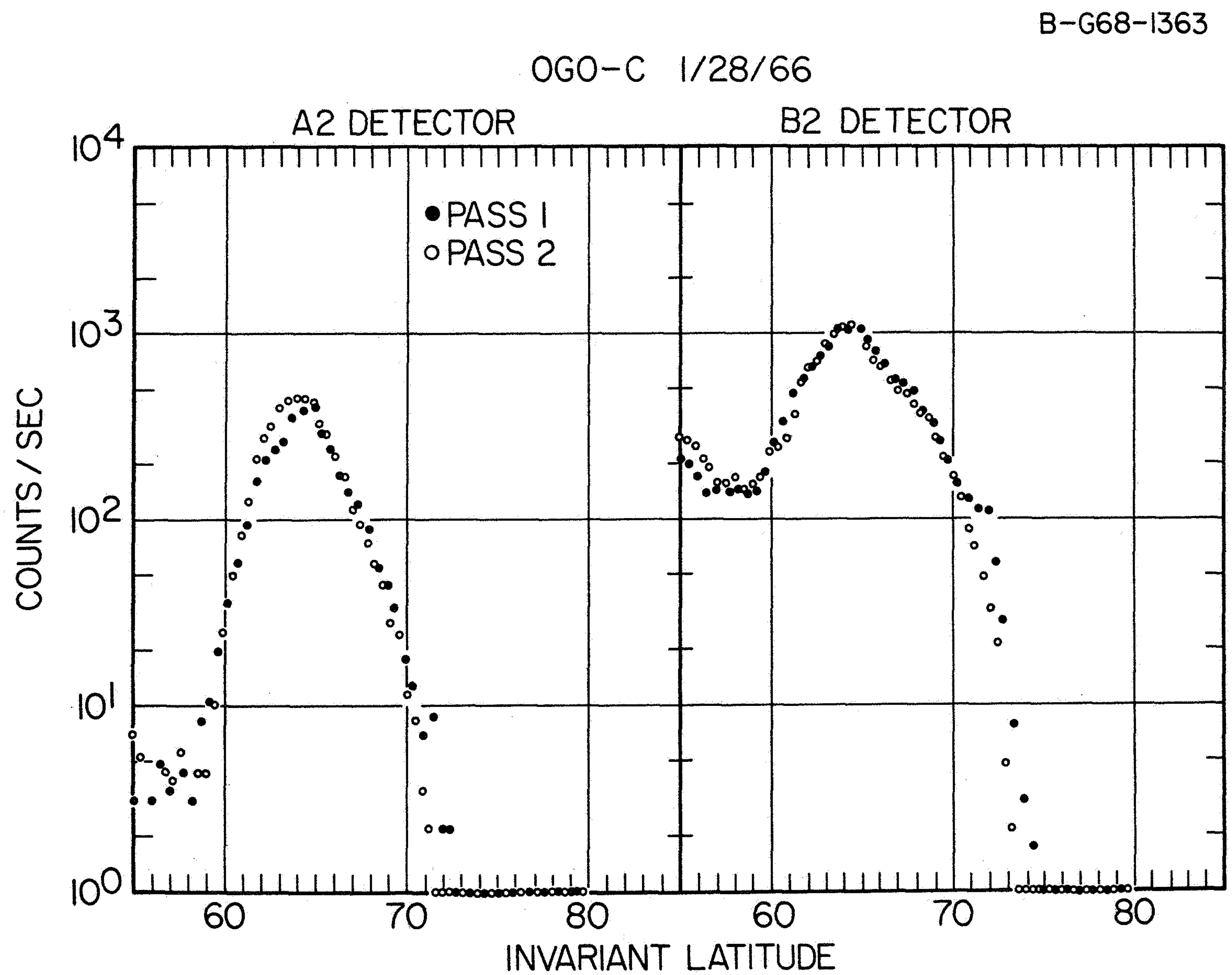
B-G68-1363
OGO-C 1/28/66
A2 DETECTOR
B2 DETECTOR
PASS 1
PASS 2
COUNTS / SEC
10^4
10^3
10^2
10^1
10^0
60
70
80
60
70
80
INVARIANT LATITUDE

Figure 4

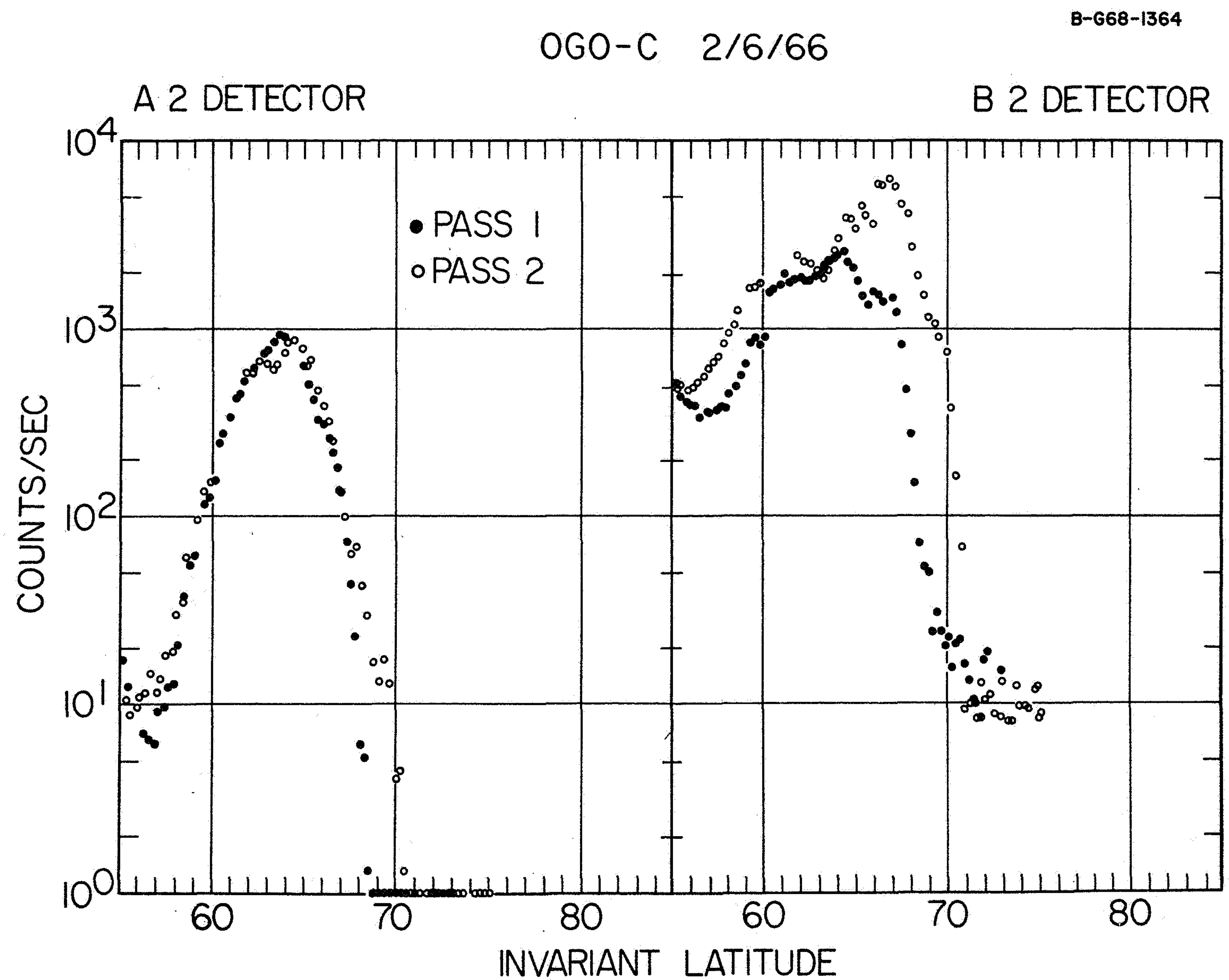
B-G68-1364
OGO-C 2/6/66
A 2 DETECTOR
B 2 DETECTOR
● PASS 1
○ PASS 2
COUNTS/SEC
10^4
10^3
10^2
10^1
10^0
60
70
80
INVARIANT LATITUDE

Figure 5

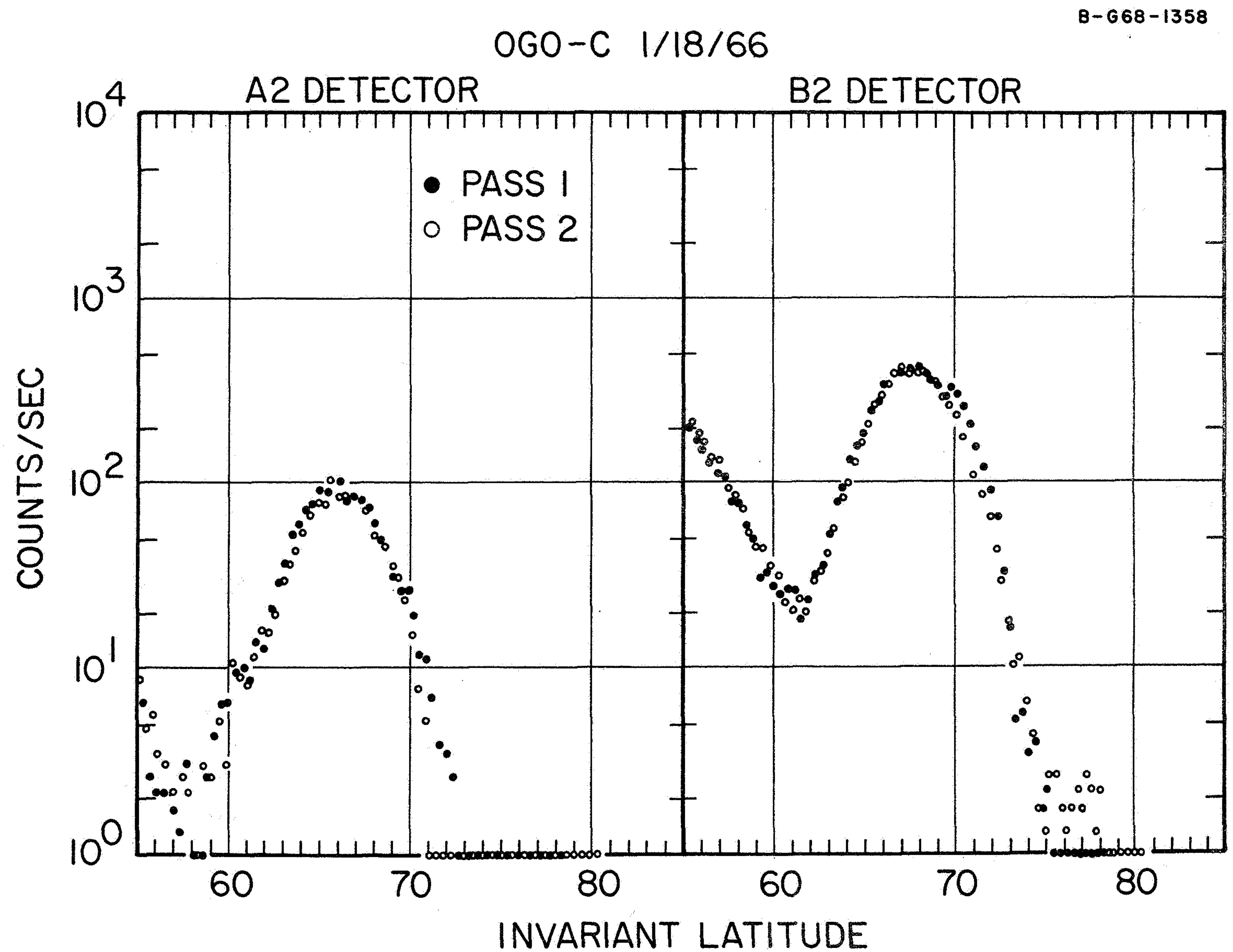
B-G68-1358
OGO-C 1/18/66
A2 DETECTOR
B2 DETECTOR
PASS 1
PASS 2
10^4
10^3
10^2
10^1
10^0
COUNTS/SEC
60
70
80
60
70
80
INVARIANT LATITUDE

Figure 6

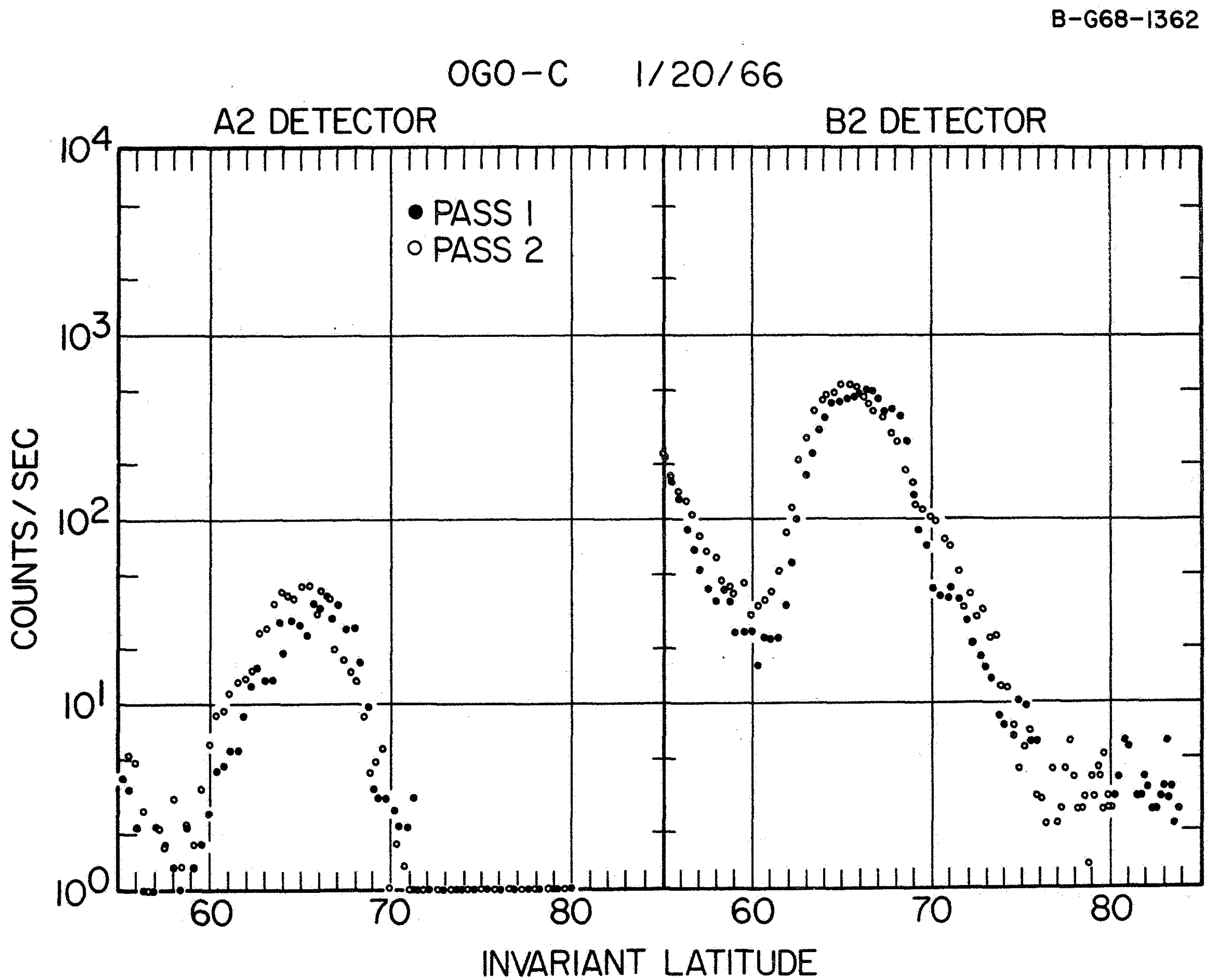
B-G68-1362
OGO-C 1/20/66
A2 DETECTOR
B2 DETECTOR
● PASS 1
○ PASS 2
10^4
10^3
10^2
10^1
10^0
COUNTS / SEC
60
70
80
60
70
80
INVARIANT LATITUDE

Figure 7

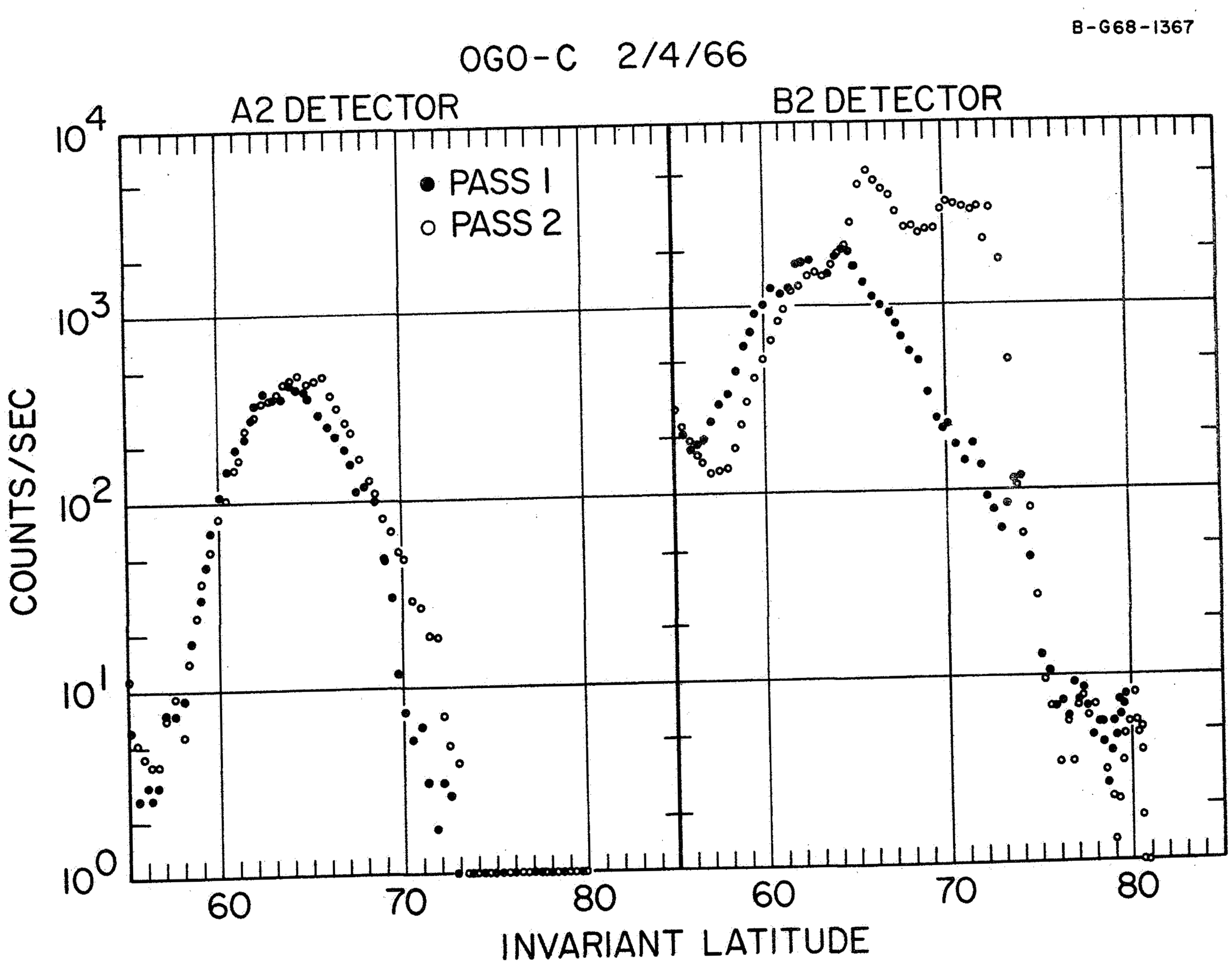
B-G68-1367
OGO-C 2/4/66
A2 DETECTOR
B2 DETECTOR
PASS I
PASS 2
COUNTS/SEC
10^4
10^3
10^2
10^1
10^0
60
70
80
INVARIANT LATITUDE

Figure 8

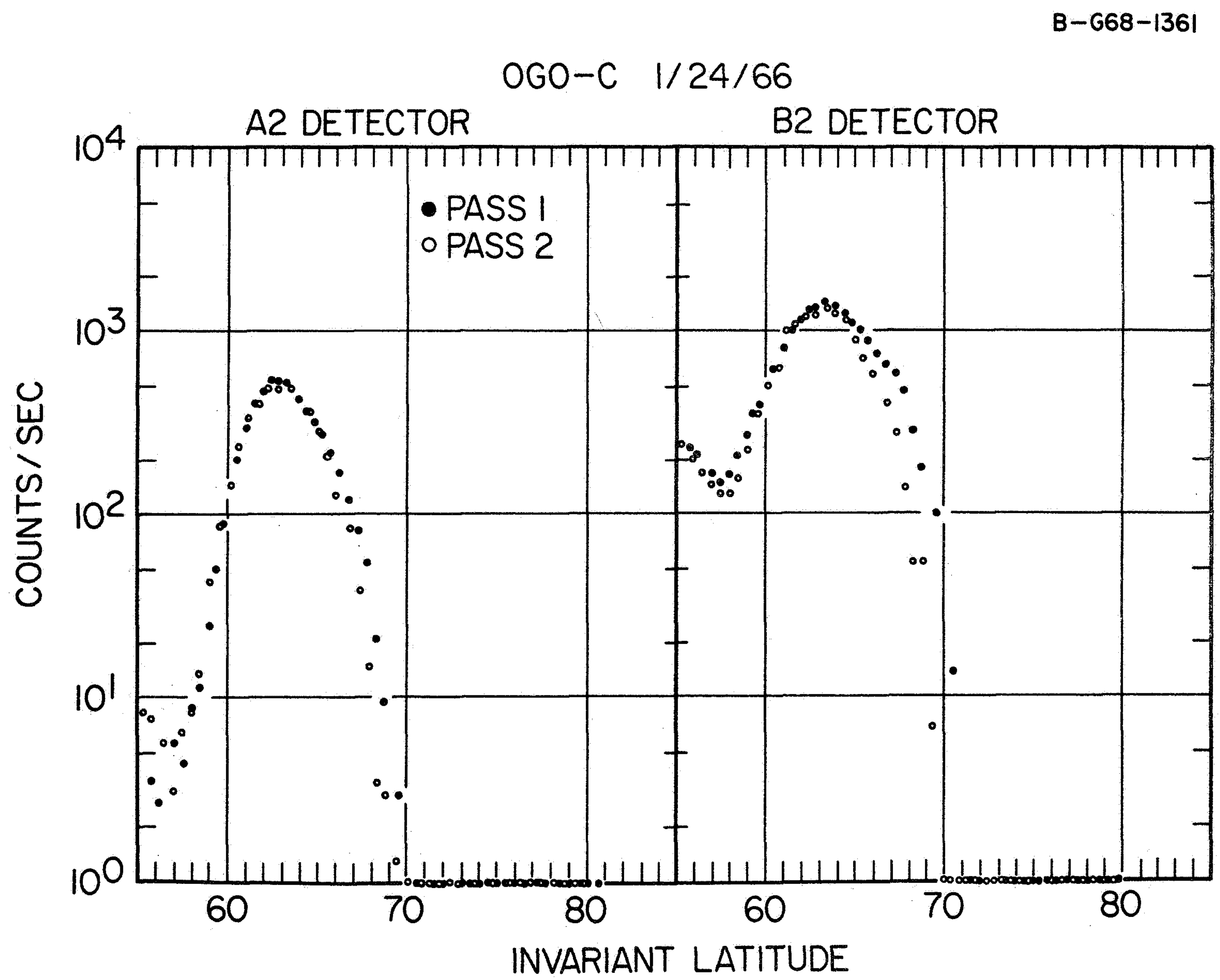
B-G68-1361
OGO-C 1/24/66
A2 DETECTOR
B2 DETECTOR
PASS 1
PASS 2
COUNTS/SEC
10^4
10^3
10^2
10^1
10^0
60
70
80
60
70
80
INVARIANT LATITUDE

Figure 9

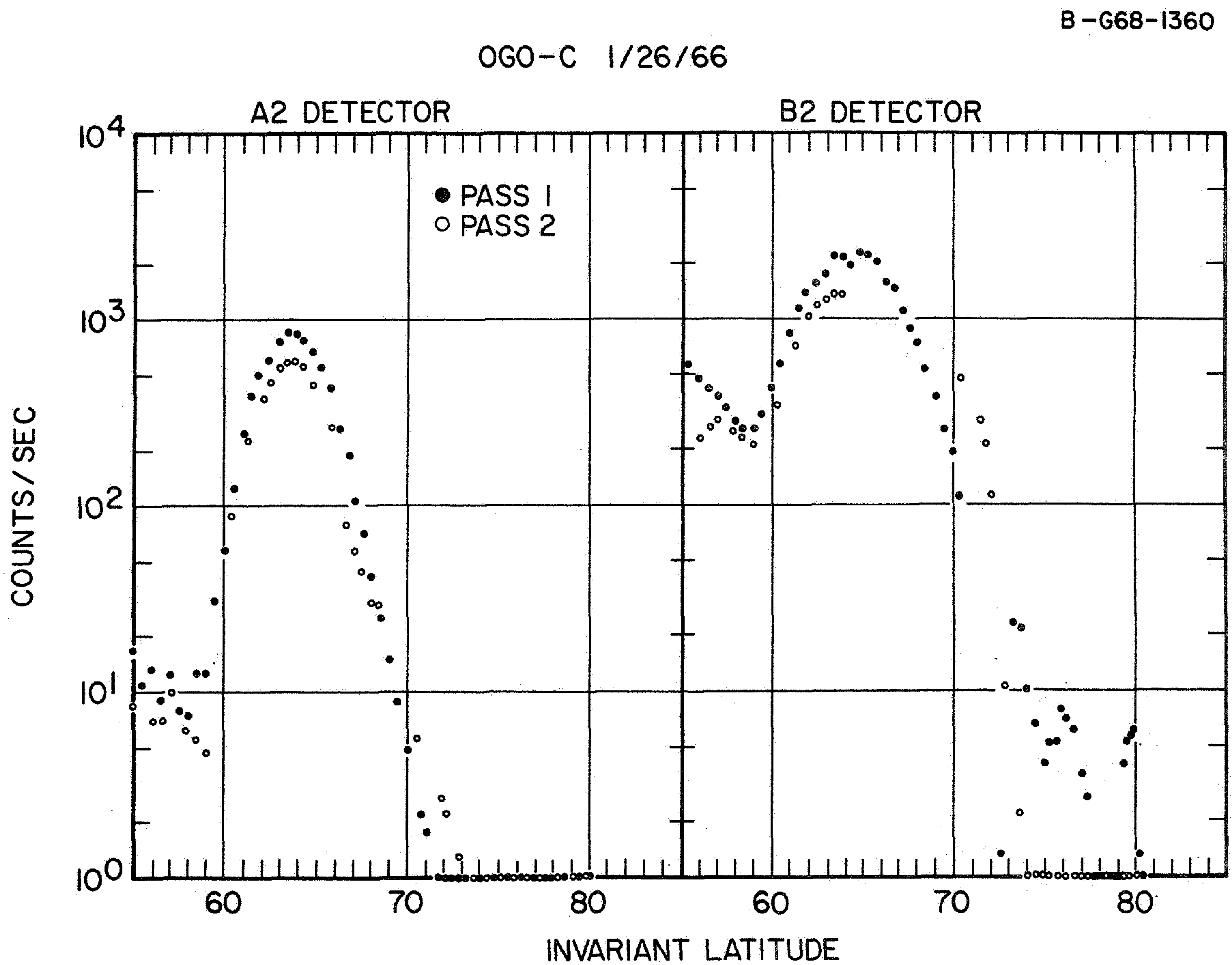
B-G68-1360
OGO-C 1/26/66
A2 DETECTOR
B2 DETECTOR
PASS 1
PASS 2
COUNTS/SEC
10^4
10^3
10^2
10^1
10^0
60
70
80
60
70
80
INVARIANT LATITUDE

Figure 10